Materials Science Forum Vols. 604-605 (2009) pp 171-178
online at http://www.scientific.net

Plastic Flow and Grain Refinement Under Simple Shear-Based Severe Plastic Deformation Processing

This paper is dedicated to Prof. Enrico Evangelista in the occasion of his 70th birthday

D. Orlov[1,3], Y. Todaka[2], M. Umemoto[2], Y. Beygelzimer[3], Z. Horita[4] and N. Tsuji[1]

[1]Department of Adaptive Machine Systems, Graduate School of Engineering, Osaka University, Osaka, 2-1 Yamada-oka, Suita, Osaka, 565-0871, Japan

[2]Department of Production Systems Engineering, Toyohashi University of Technology, Tempaku-cho, Toyohashi, Aichi 441-8580, Japan

[3]Donetsk Institute for Physics & Engineering of the National Academy of Sciences of Ukraine, 72 R. Luxembourg St., Donetsk, 83114, Ukraine;

[4]Department of Materials Science and Engineering, Faculty of Engineering, Kyushu University, Fukuoka, 819-0395, Japan

Abstract. In the present work, effects of loading scheme and strain reversal on structure evolution are studied by using high pressure torsion (HPT) and twist extrusion (TE) techniques. High purity aluminum (99.99%) was processed at room temperature up to a total average equivalent strain of ~4.8 by TE and HPT with two deformation modes: monotonic and reversal deformation with a step of 12˚ rotation. It was revealed that microstructural change with straining observed in pure Al was a common consequence of the SPD processing and was not affected significantly by the loading scheme. At the same time, it was found that strain reversal retarded grain refinement in comparison with monotonic deformation.

Introduction

Many advanced researches aimed to clarify the materials properties produced by severe plastic deformation (SPD) have been performed so far. A broad variety of metallic materials, composites and polymers were processed, which revealed most of mechanisms of structure evolution and materials' behavior during and after SPD. However, the knowledge on SPD technique itself is still limited. Not all the process variables affecting structure development have been taken into account. Therefore, commercial applications of the SPD techniques are still very limited and their further improvement is of big interest.

The present work presents a study on the effects of loading scheme and strain reversal on structure evolution in fcc metals. Reversal straining is one of the main characteristics of SPD methods since their main feature is large plastic strain accumulation without any meaningful shape change of the billet. Detailed study of this effect shall help to optimize the existing SPD methods and to develop new one. The role of deformation reversal under severe plastic deformation has been studied in few piece of works, so far [1-6]. Therefore, this work is aimed to fill this gap in knowledge. As a representative fcc system, 99.99% purity aluminum was chosen for the examination. Two kinds of SPD methods were used for this study: twist extrusion (TE) and high pressure torsion (HPT), which are shown schematically in Fig. 1 a and b, correspondingly.

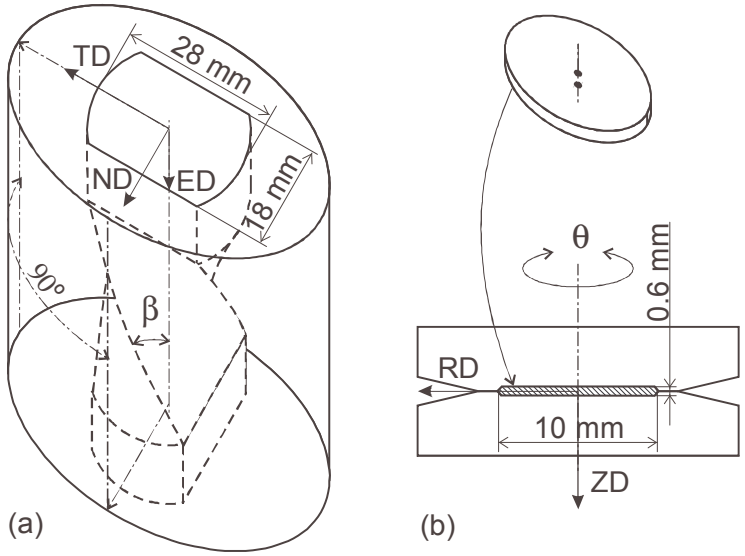

Fig. 1. Schemes of twist extrusion (a) and high pressure torsion (b) tools with definitions of the most principal dimensions and directions. The directions for TE (a): TD is transverse direction; ND is normal direction; and ED is extrusion direction. The directions for HPT are designated as follows (b): RD is radial direction; and ZD is direction of compression and axis of rotation that is considered to be parallel to ED in twist extrusion.

High pressure torsion is a technique developed from Bridgeman's anvils apparatus. It was applied first to attain large plastic deformation by Smirnova et al. [1]. After that, many researches on different materials using this technique were done. HPT was proved as the best SPD method for basic studies on structure evolution during plastic deformation to large strain values. Under high pressure torsion, a coin-shaped (typically 10 mm in diameter and up to 1 mm thickness) billet is placed between two anvils and compressed. After that, one of the anvils is being rotated around the vertical axis to a specified angle as shown in Fig. 1b. Usually it is rotated in one, e.g. clockwise, direction. In this study we used to do rotations in both clockwise/anticlockwise (CW/ACW) directions as described in details below.

Twist extrusion, on the other hand, is a relatively new SPD method that was introduced by Beygelzimer in [2,3]. This technique is still considered as a promising one, but moderately studied. Under TE processing, a prismatic billet is extruded through a "twist die". The "twist die" has a non-circular in cross-section channel with straight, helical, and again straight parts along extrusion axis as shown in Fig. 1a. This allows to accumulate plastic strain in the billet without any shape change. Recent studies showed that this technique is slightly less effective in producing ultra-fine grained structure if compared with other SPD methods [4,5]. But results of these studies contradict to expectations of mathematical simulations [3,6]. Therefore, the additional aim of this paper is to clarify reasons for this discrepancy.

Experimental Details

The as received billets of 99.99% purity aluminum were annealed at 773 K and cooled in a furnace. The billets of 18×28 mm^2 in cross-section, as shown in Fig. 1a, and 100 mm in length were twist extruded at room temperature up to 4 passes. The true strain values after TE processing were calculated from the following simplified equations [6]:

$$\varepsilon_{\min} \approx 0.4 + 0.1 \tan \beta. \qquad \varepsilon_{\max} \approx \frac{2}{\sqrt{3}} \tan \beta. \tag{1}$$

β being the angle of twist line slope at the corner edge on the channel cross-section as defined in Fig. 1a. For a constant angle of the cross-section rotation, 90˚ (Fig. 1a), deformation per TE pass could be controlled by the angle of the twist line slope β and corresponding change in the helical part length. In this study, β=60˚ (Fig. 2a) was used and thus, the average true strain per 1 TE pass is estimated as $\varepsilon_{ave} \approx 1.2$ [6] ($\varepsilon_{min} \approx 0.57$; $\varepsilon_{max} \approx 2$); accordingly, after 4 passes it comes to $\varepsilon_{ave} \approx 4.8$ ($\varepsilon_{min} \approx 2.3$; $\varepsilon_{max} \approx 8$).

Under twist extrusion processing, deformation is primarily defined by the angle of the twist line slope and is principally reversal [3, 6]. As was shown earlier in [3, 6], the deformation takes place in one direction (e.g. clockwise) upon entering the helical part of the channel and in opposite direction (e.g. anticlockwise) upon exiting this part. Areas of the most intensive deformation during TE processing are shown in Fig. 2a with arrows.

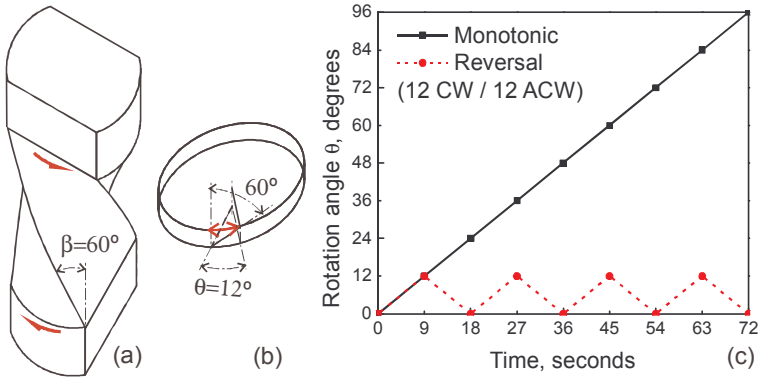

Fig. 2. Principal schemes of the deformation routes by TE (a) and HPT (b) used in this study; and diagram showing the routes under HPT processing (c). CW is clockwise, and ACW is anticlockwise directions of rotation.

The billets of 10 mm in diameter and 0.6 mm thickness as illustrated in Fig. 1b were processed by high pressure torsion in the stress-strain conditions similar to TE up to the comparable total strain values with two deformation modes: reversal and monotonic as shown in Fig. 2c. The equivalent strain values under HPT were estimated from the following simple equation:

$$\varepsilon \approx \frac{1}{\sqrt{3}} \frac{r}{h} \theta. \qquad (2)$$

r and h being the HPT billets' radius and thickness respectively and θ is the angle of rotation in radians. Under the specified processing conditions, equivalent strain varied from $\varepsilon_{min} \approx 0$ on the billet axis to $\varepsilon_{max} \approx 2$ on the billet edge after 1 HPT cycle, and correspondingly from $\varepsilon_{min} \approx 0$ to $\varepsilon_{max} \approx 8.1$ after 4 HPT cycles. The one cycle of the reversal deformation under HPT (comparable to 1 TE pass) was considered to be finished after 12˚ rotation in clockwise direction followed with 12˚ rotation in anticlockwise direction.

The stress-strain conditions for the both processing methods considered to be similar, since (1) the deformation was mostly imposed by simple shear in the plane parallel to ZD/ED axes; (2) under reversal deformation during HPT, amplitude of the rotations per step was chosen as 12˚. This angular value gave the angle of originally vertical line slope on the billet's outer edge 60˚, the same as that used for TE processing (Fig. 2a,b). To study the effect of the strain reversal directly, monotonic rotations up to 96˚ (that is comparable to 4 TE passes) in clockwise direction was also employed.

The structure characterizations were performed at different length scales by optical microscopy, electron backscattered diffraction (EBSD) analysis, and transmission electron microscopy (TEM). For optical microscopy, specimens were cut in the sections perpendicular to the extrusion/rotation axes by an abrasive saw, grinded and polished mechanically, and finally anodized in Barker's

reagent. The observations were conducted in polarized light on Nikon ECLIPSE ME600L and Olympus BX60MF5 optical microscopes equipped with digital cameras. Optical micrographs of selected areas were captured by digital camera and then combined to obtain macrostructure pattern of the whole sections. For EBSD analysis, the same planes of the same specimens were grinded mechanically and electro-polished in perchloric-based aqua solution. Observations were conducted on Hitachi S-4300SE and Phillips FEI Sirion FE-SEMs equipped with TSL orientation imaging microscopy systems. Samples for TEM were prepared by twin-jet electro-polishing in the perchloric-based aqua solution. The TEM observations were done on Hitachi H-800 and Phillips Tecnai-20 transmission electron microscopes operating at an accelerating voltage of 200 kV. Low angle boundaries (LABs) were defined as boundaries having misorientations in the range 2°-15°; high angle boundaries (HABs) were the ones ≥15°.

Results

Structure of the initial billets in as-annealed condition consisted of well defined equiaxed grains as shown in Fig. 3a-f. Some structural inhomogeneity in grain sizes inherited from preliminary processing could be seen. Average grain size of this structure was defined as ~280 μm.

Low strain level (1 TE pass and equivalent HPT processing). Reversal deformation for 1 CW/ACW HPT cycle with 12˚ rotation amplitude, as shown in Fig. 3b, led to formation of very heterogeneous structure: original grains in vicinity of the billet axis looks to be almost non-deformed and still clearly distinguishable; but peripheral areas are not the same but unclear. There is inhomogeneous grey contrast along the outer edge so that the original grains can rarely be distinguished. Monotonic deformation for 24˚ rotation by HPT, see Fig. 3c, resulted in less heterogeneous structure: almost whole area of the billet cross-section has grey contrast and can not be resolved optically; some inhomogeneity of the structure in tangential direction might be attributed to imperfection (e.g. axial and angular misalignments) of the HPT facility used in this study.

Appearance of the grey contrast suggests intensive development of dislocation substructure with subgrains formation. TEM observations showed the formation of dense dislocation walls and low angle boundaries. Depending on the radial distance from the billet center, cell sizes do not differ much, but most of the deformation induced cell boundaries, especially in vicinity of the torsion axis, are still diffuse. In the better statistical representation, these results are illustrated from EBSD analysis in Fig. 4a-c.

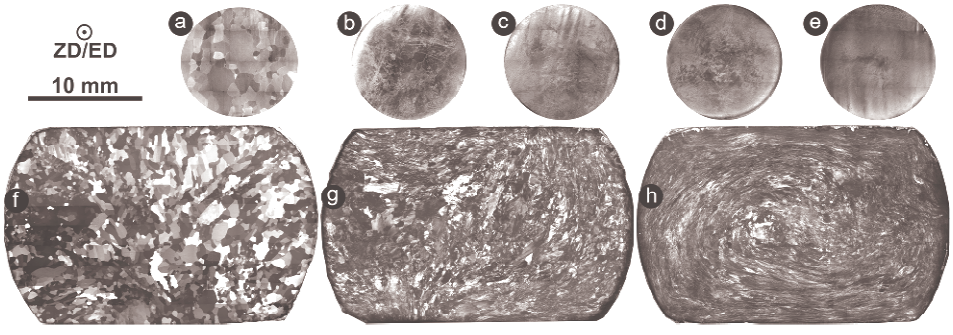

Fig. 3. Optical micrographs illustrating macrostructure evolution in 99.99% Al from as-annealed (a), (f) to severely plastically deformed: by HPT for 1 (b) and 4 (d) cycles of reversal rotation, for 24˚ (c) and 96˚ (e) of monotonic rotation; by TE for 1 (g) and 4 (h) passes.

It could be seen that the both deformation modes difference between structural characteristics on this level of strain is very minor. The subgrain sizes do not significantly vary with radial distance. These are ~1.1 μm for the reversal mode of deformation and slightly higher, ~1.2 μm, for the monotonic one. Note that in the vicinity of the billet axis, amount of cells surrounded by boundaries with ≥2˚ misorientation is very small and is even not shown for the monotonic mode of deformation.

Average angle of misorientations, as well as fraction of high angle boundaries, increases monotonically with radial distance from the billet axes toward the edges for the both deformation modes. The average angle of misorientations (see Fig. 4b) is still small by absolute value, but almost two times larger on the billet axis for monotonic deformation and about the same on the edges.

For the both HPT deformation modes, there is reasonable consistency between observations on all the length scales. The structural heterogeneity is pronounced and it is proportional to the imposed net strain gradient by the loading scheme of HPT. It still reflects significant influence of crystal orientations in the initial structure at this strain level.

After 1 pass of TE, microstructure (Fig. 3g) became largely heterogeneous with the peripheral areas having darker contrast than the central one. This clearly reflects evidence of larger strain level on the edge parts of the billet compared to the axial parts. Early stages of lamellar structure formation could be seen: grains in the peripheral areas are mostly elongated in spite to rather equiaxed and still coarse grains in the billet center. Apart from that, all the grains have grey contrast and grain boundaries are not clear and evident any more. Although some areas still can be resolved optically, the grain sizes can not be large measured. Such a structure is consequence of the net flow pattern introduced by the cross-sectional geometry of the twist channel used in this study. But this flow pattern is strongly affected by heterogeneous deformation of original coarse grains.

TEM observations showed microstructure with the same appearance as after the HPT processing (cellular structure with diffusive subgrain boundaries), but with different distribution. Quantitative results of this structure, performed by using EBSD analysis are shown in Fig. 3a-c. The structural characteristics are distributed non-monotonically in radial direction after 1 TE pass. This is consistent with the macrostructure distribution, but contrast to the structure distribution after HPT processing. Average subgrain sizes are generally larger than those after the HPT processing. Depending on the radial distance, it is ~1.55 μm on the billet axis, then slightly decreases and then increases again up to ~2 μm on the billet edge. Average angle of misorientations does not vary with the radial distance, and is about the same as the average angle of misorientations on axis of the billet after HPT rotation for 24˚. In spite of total lack of high angle boundaries on the billets axis after HPT by both deformation modes, after TE processing there is ~10% of HABs on the billet axis area. The fraction of HABs decreases down to almost zero in the middle of radius area and increases again up to ~13% at the billet edge.

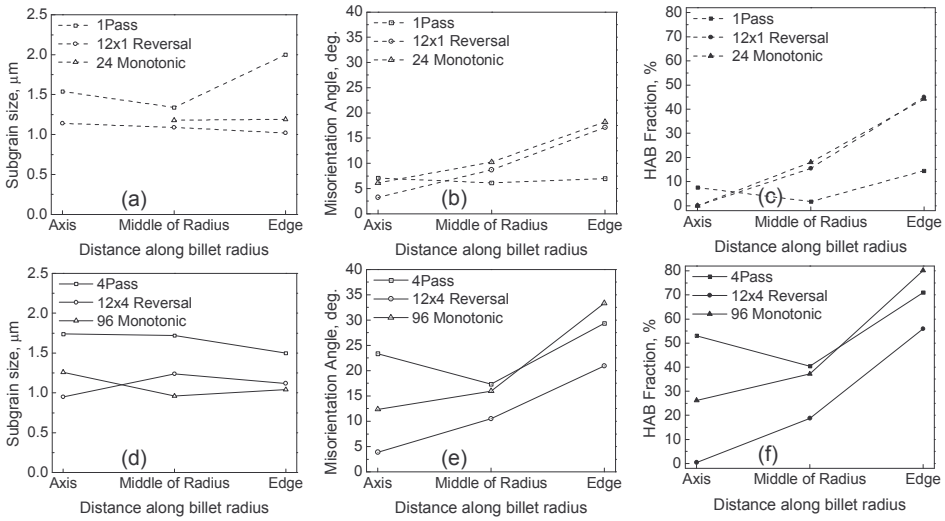

Fig. 4. Distribution of subgrain sizes (a), (d); average angles of misorientations (b), (e); and fraction of high angle boundaries (c), (f) in 99.99% Al after TE and HPT processing for low (1 TE pass and equivalent HPT processing), (a)-(c), and high (4 TE passes and equivalent HPT processing), (d)-(f), strain levels.

High strain level (4 TE passes and equivalent HPT processing). Macrostructure of the billets after 4 CW/ACW HPT cycles is shown in Fig. 3d. Even after this level of strain, it is still heterogeneous; but already most of the cross-section area has dark grey contrast and can not be resolved optically. After the monotonic deformation by HPT for 96˚ rotation, almost whole the billet cross-section area (see Fig. 3e) has homogeneous dark grey contrast and is not resolved optically. An exemption is narrow area in vicinity of the billet axis. TEM observations showed almost free of dislocations equiaxed subgrains surrounded by very well defined boundaries at the billets edges for the both HPT deformation modes. In vicinity of the billets axis, the subgrain sizes are nearly the same to the edges, but the subgrain boundaries are thick with stacked dislocations nearby. This confirms lesser, but non-zero, amount of strain introduced on the billets axis.

Statistically meaningful data from EBSD analysis illustrated in Fig. 4d-f show no principal change in the character of the structural characteristics distributions in comparison with the low strain level. Very small variation, within ~1-1.2 μm, in average subgrain sizes depending on radial distance could be seen in Fig. 4.d for the both HPT deformation modes. Reversal processing resulted in negligibly small change in the average angle of misorientations (Fig. 4e) and HABs fraction (Fig. 4f) for the axis area; and rather small, up to ~20%, increase in these characteristics with the radial distance to the billet's edge. Nevertheless, monotonic deformation by HPT led to significant increase in the average angle of misorientations (Fig. 4e) and HABs fraction (Fig. 4f) in vicinity of the billet axis and almost 2 times increase in these characteristics at the outer edge. The peripheral areas are dominated by high angle boundaries, while the billet center is still dominated by low angle boundaries. So that up to this level of strain, the significant heterogeneity in the microstructure proportional to the net strain gradient was still kept.

After 4 passes of twist extrusion the material's structure (Fig 3h) appears as continuous development formed during the first TE pass. Much narrower lamellas than after 1 TE pass could be seen in the most of the cross-sectional area. The lamella fibers are patterned in clear vortex-like flow. Overall very dark contrast suggests formation of heavily deformed. But still heterogeneous structure exists because the contrast is slightly lighter in the billet central area. The billet was highly strained at the outer edge and less at the center. The subgrain sizes become so small that the pattern of plastic flow is affected by the TE tool geometry only. Separate subgrains, as well as the subgrain boundaries, can not be resolved optically.

As could be seen from EBSD analysis in Fig. 4d-f, the average subgrain sizes developed after the first TE pass did not change significantly. Their distribution just became more homogeneous with average size ~1.6 μm. Similar to the structure evolution under HPT processing, the microstructure developed mostly by increasing in the subgrain boundary misorientations and there was no principal change in the character of the structural characteristics in comparison with 1 TE pass. Both the average angle of misorientations (Fig. 4e) and the HABs fraction (Fig. 4f) increased for few times, so that in the resulting structure, fraction of high angle boundaries became more than 50% at the center areas and slightly more than 70% at the outer edge areas of the billet.

Discussion

The results shown so far revealed that at early stages of severe plastic deformation, regardless of loading scheme, plastic flow of the material is affected by two factors: field of velocities imposed by SPD tool geometry and local crystal orientations. Plastic flow at later stages of the processing is mostly dominated by the field of velocities.

Plastic flow during the twist extrusion processing might be characterized by the two principal processes: formation of vortex-like flow with large strain gradient; stretching in one direction (and corresponding shrinkage in orthogonal) of material particles and their mixing. The particles stretching increase with subsequent TE passes. The formation of stable lamellar flow pattern was more apparent as number of TE passes increased. HPT processing did not show similar behavior. The described capability for the severe mixing is a unique property of twist extrusion. In addition to grain refinement, this property might be useful for homogenization of composite materials, intensification of mechano-chemical reactions, etc. In this study, the mixing capability led to more

homogeneous structure distribution in TE; in spite of the similarity between loading schemes of HPT and TE.

The structure of 99.99% purity Al was significantly refined but heterogeneous at low strain level (after monotonic high pressure torsion for 24˚, or 1 cycle of reversal HPT for 12˚ in CW/ACW directions; or 1 pass of twist extrusion). Even after the processing to high strain levels (corresponding monotonic to 96˚ or reversal for 4 cycles HPT or 4 TE passes) the subgrain boundary misorientations increased, but the microstructure still retained heterogeneous. This is attributed to significant net strain gradient imposed by the SPD tool geometry used in this study and to reversal loading.

Irrespective of the processing method used, two processes of structure evolution in pure aluminum were observed: first, development of the deformation-induced grain boundaries and second, a continuous increase in the misorientations. Initially, the first process dominates developing deformation-induced boundaries. The boundaries occur heterogeneously in the billet volume according to net strain gradient imposed by tool geometry and local flow fields. The boundary spacing converges to a lower limit. Thereafter, the formation of new boundaries saturates and the second process of the boundary misorientation increase becomes dominant. Low angle boundaries formed at the first stage, continuously convert into high angle boundaries: subgrains with low angle boundaries eventually became high angle boundarys grains.

Minimum subgrain size was reached already after the first step of the SPD processing (~1.6 μm for TE and ~1.1 μm for HPT). Further processing led to increase in the subgrain misorientations only.

Conclusions

Plastic flow and grain refinement in 99.99% purity Al under severe plastic deformation processing by high pressure torsion and twist extrusion were studied. Micro-structural change in pure Al is a common consequence of application of two different SPD processes (TE and HPT) and is not significantly affected by the loading scheme. There are two processes of structure evolution in pure aluminum: first, development of the deformation-induced grain boundaries and second, a continuous increase in the grain misorientations.

The minimum reached subgrain size in this study was of ~1.6 μm for TE, and of ~1.1 μm, for HPT. Distribution of the average grain sizes was almost homogeneous. But the subgrain misorientations were heterogeneously distributed for all the processing methods. The heterogeneity in the misorientations corresponds to net strain gradient introduced by each particular processing method. Among all the SPD methods used in this study, the most homogeneous structure was obtained by twist extrusion due to specific flow field imposed by the tool geometry.

In comparison with monotonic mode of deformation, reversal deformation retarded grain refinement.

Acknowledgements

This work was supported in part by the Light Metals Educational Foundation of Japan; in part by the 21st COE program “Functional Innovation of Molecular Informatics” and Global COE program “Center of Excellence for Advanced Structural and Functional Materials Design”, and in part by a Grant-in-Aid for Scientific Research on Priority Areas “Giant Straining Process for Advanced Materials Containing Ultra-High Density Lattice Defects”, all from the Ministry of Education, Culture, Sports, Science and Technology, Japan. The Office of Naval Research Global (ONRG) is greatly acknowledged for his partial support for the participation at the conference through the grant number N00014-08-1-1011.

References

[1] N.A. Smirnova, V.I. Levit, V.I. Pilyugin, R.I. Kuznetsov, L.S. Davydova, V.A. Sazonova: Fiz. Met. Metalloved Vol. 61 (1986), p. 1170

[2] Y.Y. Beygelzimer, V.N. Varyukhin, S.G. Synkov, A.N. Sapronov, V.G. Synkov: Physics and Technology of High Pressures Vol. 9 (1999), p. 109

[3] Y. Beygelzimer, D. Orlov, V. Varyukhin: A New Severe Plastic Deformation Methd: Twist Extrusion, 2002 TMS Annual Meeting and Exhibition, Seattle, Washington, USA, February 17-21 (2002), p. 297

[4] M. Berta, D. Orlov, P.B. Prangnell: International Journal of Materials Research Vol. 98 (2007), p. 200

[5] D. Orlov, Y. Beygelzimer, S. Synkov, V. Varyukhin, Z. Horita: Materials Transactions Vol. 49 (2008), p. 2

[6] Y. Beygelzimer, V. Varyukhin, D. Orlov, S. Synkov: Twist extrusion – process for strain accumulation, Donetsk: TEAN (2003), p. 87.